Non-canonical NF-κB signaling in dendritic cells promotes intestinal inflammation by restraining the tolerogenic β-catenin-Raldh2 axis

Alvina Deka[1,*], Naveen Kumar[1,*], Meenakshi Chawla[1], Namrata Bhattacharya[2,3], Sk Asif Ali[1], Swapnava Basu[1], Bhawna[1], Upasna Madan[4], Shakti Kumar[4], Bhabatosh Das[4], Debarka Sengupta[2], Amit Awasthi[4], Soumen Basak[1,✉]

[1]Systems Immunology Laboratory, National Institute of Immunology, Aruna Asaf Ali Marg, New Delhi-110067, India
[2]Indraprastha Institute of Information Technology, Delhi, India
[3]Australian Prostate Cancer Research Centre—Queensland, Institute of Health and Biomedical Innovation, School of Biomedical Sciences, Queensland University of Technology (QUT), Brisbane, Queensland, Australia
[4]Translational Health Science and Technology Institute, Faridabad, India

* These authors have contributed equally to the work

✉Correspondence should be addressed to S.B.;
e-mail: sobasak@nii.ac.in; tel: (91) (11) 26703853; fax: (91) (11) 2674262

Running Title: noncanonical NF-κB signaling in DCs fuels gut inflammation

Keywords: IBD, colitis, DCs, RelB, *Nfkb2*, β-catenin, Axin1, Raldh2, retinoic acid, tolerogenic, Tregs, sIgA, microbiome, vitamins;

Abstract

Dendritic cell (DC) dysfunctions exacerbate intestinal inflammation; however, the underlying mechanism remains unclear. The non-canonical NF-κB pathway activates the RelB:p52 heterodimer, which plays immunoregulatory roles in DCs. Curiously, genetic studies have associated this pathway with inflammatory bowel disease (IBD). We found that intestinal DCs from IBD patients possessed heightened non-canonical NF-κB signaling and that genetic inactivation of RelB:p52 in DCs alleviated experimental colitis in mice. Unexpectedly, RelB:p52 deficiency diminished transcription of Axin1, a critical component of the β-catenin destruction complex, thereby reinforcing the tolerogenic β-catenin-Raldh2-retinoic acid axis in DCs. Indeed, DC-specific non-canonical NF-κB impairment in mice improved the colonic frequency of Tregs and IgA^+ B cells, which fostered luminal IgA and the gut microbiome. Introducing β-catenin haploinsufficiency in non-canonical NF-κB-deficient DCs moderated this tolerogenic mechanism, reinstating the colitogenic sensitivity in mice. In sum, we illustrate a DC network that integrates immune signaling and micronutrient metabolic pathways to tune intestinal inflammation.

Highlights

- Aberrant intestinal inflammation is associated with and exacerbated by non-canonical NF-κB signaling in DCs.
- Non-canonical signaling restrains the tolerogenic β-catenin-Raldh2 axis in DCs by upregulating Axin1.
- DC-specific RelB:p52 impairment promotes β-catenin-dependent Treg accumulation in the gut.
- A DC defect of non-canonical signaling causes β-catenin-dependent increase in luminal sIgA, fostering the gut microbiome.

Introduction

DCs orchestrate the balance between protective immune responses against pathogens and tolerance towards commensal microbes in the intestine. Upon microbial sensing, activated DCs produce a myriad of immunogenic cytokines, including IL-6, IL-12, and IL-23, which promote IFNγ-secreting Th1 and IL-17-secreting Th17 cells. These effector T cells direct inflammatory responses, containing gut infections. DCs also produce tolerogenic cytokines, such as IL-10 and TGFβ. In addition, mucosal DCs synthesize retinoic acid (RA) from dietary vitamin A or retinol[1]. These immunomodulatory factors support the generation and maintenance of inflammation-suppressive $FoxP3^+$ Tregs and promote their gut homing. Furthermore, DC-derived RA and IL-10 enhance immunoglobulin class switching, accumulating IgA-secreting plasma B cells in the intestine[2,3]. While secretory IgA (sIgA) in the gut lumen protects from opportunistic gut pathogens, sIgA coating also shapes the gut microbiome in symbiosis with the host[4,5]. Thus, by calibrating mucosal responses, DCs ensure gut homeostasis.

Not surprisingly, distorted DC functions have been implicated in

aberrant intestinal inflammation. Ulcerative colitis (UC), a form of IBD, was associated with a marked reduction in the CD103$^+$ DC subset in the intestine[6]. Colonic DCs from IBD patients or mice subjected to experimental colitis were inept at synthesizing TGFβ and RA [6,7]. These DCs were also less proficient in generating Tregs and instead promoted Th1 and Th17 cells. Accordingly, DC-specific ablation of RXRα, an RA-activated transcription factor, aggravated colitis in mice by depleting intestinal Tregs[8] . Similarly, CD137 signaling restricted colitis in mice by upregulating RA synthesis in DCs that altered T cell homeostasis in the intestine[9]. Furthermore, vitamin A deficiency exacerbated colitis in mice by decreasing the colonic abundance of IgA-secreting cells[10]. Notably, IgA-coated gut microbes from healthy individuals provided protection, while those from IBD patients sensitized mice to experimental colitis[11,12]. These studies underscore the importance of DCs in restraining aberrant intestinal inflammation. The NF-κB system comprises two interlinked canonical and non-canonical signaling arms, which play important roles in the differentiation, survival, and functioning of DCs. In particular, the canonical NF-κB pathway mediates microbial signal-responsive nuclear translocation of RelA- and cRel-containing NF-κB transcription factors, which induce the expression of immunogenic cytokines, including IL-1β, IL-12, and IL-23, in DCs[13]. Previous studies suggested that the activation of canonical NF-κB signaling in DCs worsens experimental colitis in mice[14].

On the other hand, the non-canonical NF-κB pathway is activated by a subset of TNFR superfamily members, including lymphotoxin-β receptor (LTβR), GM-CSFR, and CD40[15]. In this pathway, NF-κB inducing kinase (NIK)-dependent phosphorylation promotes processing of the NF-κB precursor protein p100 into the mature p52 subunit, leading to nuclear accumulation of RelB:p52. In a non-redundant manner to the canonical pathway, non-canonical NF-κB signaling in DCs induces the expression of IL-23, which drives Th17 responses[16,17]. NIK function in DCs was implicated in the pathogenic Th17 response underlying epidermal damage in the mouse model of psoriasis[18]. DC-intrinsic role of NIK and RelB also restricted Treg accumulation in the central nervous system in the mouse model of experimental autoimmune encephalomyelitis (EAE)[17,19]. In the intestine, NIK-dependent IL-23 expression by DCs was important for Th17-mediated immune controls of *Citrobacter rodentium*[20]. As such, NIK in DCs promoted pIgR expression in IECs involving Th17-secreted IL-17 that maintained luminal IgA levels and a gut-protective microbiome. Interestingly, *LTBR* and *NFKB2* were linked in a genome-wide association to the susceptibility loci for IBD[21]. Despite that, a plausible DC-intrinsic role of the non-canonical RelB:p52 NF-κB pathway in intestinal pathologies remains unclear.

Here, we report that human IBD and experimental colitis in mice are associated with intensified non-canonical NF-κB signaling in intestinal DCs. Genetic disruption of this pathway in DCs alleviated chemical-induced colitis in mice. Our mechanistic studies suggested that RelB:p52 transcriptionally upregulated the expression of Axin1, which tethers β-catenin to its destruction complex. Inactivation of non-canonical NF-κB signaling reinforced the β-catenin-mediated expression of Raldh2, which promotes tolerogenic RA synthesis by DCs[22]. Ablating *Relb* or *Nfkb2* in DCs not only increased the frequency of intestinal Tregs but also improved the abundance of colonic IgA$^+$ B cells, which fostered luminal IgA and the gut microbiome. Finally, haploinsufficiency of β-catenin in DCs lacking

non-canonical NF-κB signaling reinstated colitogenic sensitivity in the composite knockout mice. Taken together, we chart a novel crosstalk between the non-canonical NF-κB pathway and the tolerogenic β-catenin-Raldh2 axis in DCs in tuning intestinal inflammation.

Results

Activation of the non-canonical NF-κB pathway in intestinal DCs from IBD patients and colitogenic mice

To decipher if intestinal pathologies are linked to non-canonical NF-κB signaling in DCs, we analyzed publicly available single-cell RNA-seq data generated using colon biopsies from 18 IBD patients and 12 healthy individuals[23]. Compared to non-IBD controls, IBD patients displayed a substantially elevated level of *RELB* and *NFKB2* mRNAs encoding non-canonical NF-κB signal transducers in intestinal DCs (Figure 1A-1B). This was also associated with an increased frequency of DCs expressing these mRNAs. Based on a previously described bulk transcriptomics study involving RelB-deficient mouse DCs[16], we deduced a panel of five top RelB-important genes - *Fgr*, *Top1*, *Crk*, *Gpd2* and *Cript* - that were also less reliant on other NF-κB factors for their expressions. We then determined the abundance of corresponding mRNAs as a surrogate of non-canonical NF-κB activity in intestinal DCs. Interrogating single-cell data indeed revealed augmented DC expressions of *FGR*, *TOP1*, *CRK1* and *CRIPT* mRNAs in IBD patients that were associated with an increased frequency of particularly FGR mRNA-expressing DCs in the intestine (Figure 1C). *GPD2* mRNA was not detectable in intestinal DCs from either healthy or diseased subjects. Our analyses established that IBD patients with prevailing inflammation maintained heightened non-canonical NF-κB signaling in intestinal DCs.

We further asked if the onset of intestinal inflammatory pathologies in mice was associated with strengthening non-canonical NF-κB signaling in DCs. To this end, we focused on the early intestinal inflammation triggered in mice subjected to dextran sodium sulfate (DSS)-induced acute colitis[24] (Figure S1A). Analyzing previously described single-cell RNA-seq data, we could demonstrate the presence of *Relb* or *Nfkb2* mRNA-expressing intestinal DCs (Figure 1D-1E, Figure S1B-S1C) which basally expressed *Fgr*, *Top1*, and *Cript* even prior to DSS treatment of mice (Figure 1F). Initiation of acute colitis coincided with a rise in *Relb* and *Nfkb2* mRNA levels in these DCs between day 3 and day 6 (Figure 1D-1E). We also observed an increase in the frequency of intestinal DCs expressing these mRNAs upon DSS treatment (Figure 1E). Moreover, DSS treatment enhanced the expression of *Fgr*, *Top1*, and *Cript* in intestinal DCs and caused an increase in the frequency of cells expressing these mRNAs (Figure 1F). *Crk* mRNA was rather insignificantly present in DCs from the mouse gut. These studies implied DC-intrinsic non-canonical NF-κB signaling in experimental colitis. To directly demonstrate non-canonical NF-κB activation in intestinal DCs, we harvested DCs from gut-draining mesenteric lymph nodes (MLNs) as $CD11c^{+}CD64^{-}MHCII^{high}$ cells and performed immunoblot analysis to capture the abundance of p52 in relation to p100 in our experiments. Intestinal DCs from untreated mice displayed

basal processing of p100 into p52, a hallmark of non-canonical NF-κB signaling (Figure 1G). DSS treatment further augmented p100 processing in these DCs in colitogenic mice. We infer that intestinal DCs possess basally active non-canonical *Relb-Nfkb2* pathway and that aberrant inflammation is associated with intensified non-canonical NF-κB signaling in IBD patients and colitogenic mice.

Non-canonical *Relb-Nfkb2* signaling in DCs exacerbates inflammatory pathologies in colitogenic mice

Next, we asked if the non-canonical NF-κB pathway in DCs actually fueled colitogenic pathologies. Therefore, we generated *Relb*$^{\Delta CD11c}$ mice with DC-specific RelB deficiency by crossbreeding *Relb*$^{fl/fl}$ mice with CD11c-Cre^{+} mice (Figure S1D) and subjected these mice to experimental colitis. Acute DSS challenge for 7 days led to up to 20% bodyweight loss in littermate *Relb*$^{fl/fl}$ controls, accompanied by severe colon shortening, and pervasive epithelial disruption associated with edema and leukocyte infiltration (Figure 2A-2C). *Relb*$^{\Delta CD11c}$ mice presented significantly less reduction in bodyweight over the course of DSS treatment and a modest decrease in colon length with a relatively intact epithelium at day 5 (Figure 2A-2C). The intestinal epithelial architecture of untreated *Relb*$^{fl/fl}$ and *Relb*$^{\Delta CD11c}$ mice was histologically indistinguishable. We further assessed the intestinal barrier permeability of these mice by measuring serum concentrations of orally administered fluorescein isothiocyanate (FITC)-dextran. Compared to a sharp 10.6-fold rise in controls, DSS treatment produced a meagre 5.2-fold increase in the serum FITC-dextran concentration in *Relb* $^{\Delta CD11c}$ mice, indicating an improved barrier function in knockouts (Figure 2D). Similarly, our gene expression analyses revealed that DC-specific RelB deficiency restrained DSS-induced expressions of inflammatory genes, including those encoding IL-1β and CXCL10, in the colon (Figure 2E). Therefore, RelB deficiency in DCs moderated inflammation and acute colitis in mice.

The coordinated functioning of proteins encoded by *Relb* and *Nfkb2* transduces non-canonical NF-κB signals. Compared to *Nfkb2*$^{fl/fl}$ controls, however, *Nfkb2*$^{\Delta CD11c}$ mice displayed only subtly improved bodyweight phenotype upon acute DSS treatment (Figure S1E-S1F). Interestingly, cyclical challenges with a low dose of DSS in the chronic chemical colitis regime resulted in a significantly less bodyweight reduction and colon shortening in *Nfkb2*$^{\Delta CD11c}$ mice at the end of the third cycle on day 63 (Figure 2F-2G). It has been reported that an alternate RelB:p50 heterodimer functionally compensates, albeit partially, for the absence of RelB:p52 activity in *Nfkb2*-deficient cells[25]. We reasoned that the molecular redundancies between RelB NF-κB factors obscured the phenotypic penetrance of *Nfkb2*$^{\Delta CD11c}$ mice in the acute colitis regime and that repeated DSS exposure unmasked colitis-resilient phenotypes in these mice because of exaggerated DC-mediated immune reactions in the chronic regime[26]. Overall, we conclude that non-canonical NF-κB signaling in DCs exacerbates inflammatory intestinal pathologies in mice.

Non-canonical NF-κB signaling restrains tolerogenic Raldh2 activity in DCs

To mechanistically understand the immunomodulatory functions of non-canonical NF-κB signaling, we set out to examine bone marrow-derived dendritic cells (BMDCs) from

WT or knockout mice (Figure S2A). Our culture condition produced ~ 85% CD11c$^+$ BMDCs by day 9 that were associated with increased processing of p100 into p52 and elevated nuclear RelB and p52 levels (Figure 3A, Figure S2B). Our RNA-seq studies demonstrated that ablation of this constitutive non-canonical NF-κB signaling in *Nfkb2*$^{-/-}$ BMDC modified global gene expressions basally (Figure S2C). RA metabolism emerged as one of the top-ranking DC-relevant biological pathways enriched among genes differentially expressed between WT and *Nfkb2*$^{-/-}$ BMDCs (Figure 3B). Concordantly, our gene set enrichment analysis (GSEA) revealed a significant enrichment of RA targets among genes whose basal expressions were augmented in *Nfkb2*$^{-/-}$ BMDCs, indicative of strengthening autocrine RA actions in knockouts (Figure 3C). Sequential action of retinol dehydrogenases (Rdh) and retinal dehydrogenases (Raldh) convert retinol to RA, which is catabolized by the Cyp26 family of enzymes[27] (Figure 3D). Further probing our RNA-seq data for the expression of genes encoding these enzymes revealed a consistently elevated mRNA level of Raldh2 in *Nfkb2*$^{-/-}$ BMDCs (Figure 3E). These studies indicated a possible role of non-canonical NF-κB signaling in transcriptionally modulating the RA pathway.

To substantiate non-canonical NF-κB-mediated control of the RA pathway, we derived BMDCs from *Relb*$^{\Delta CD11c}$ or *Nfkb2*$^{\Delta CD11c}$ mice. As expected, *ex vivo* differentiated BMDCs from *Relb*$^{\Delta CD11c}$ or *Nfkb2*$^{\Delta CD11c}$ mice produced only a minor amount of RelB or p100, respectively (Figure S2D-S2E). In comparison to corresponding gene-sufficient floxed controls, *Relb*$^{\Delta CD11c}$ and *Nkfb2*$^{\Delta CD11c}$ BMDCs both displayed a ~ 4.5-fold increase in the basal expression of Raldh2 mRNA in our RT-qPCR analyses (Figure 3F). LPS treatment did not discernably alter Raldh2 mRNA levels in WT or knockouts. In contrast, basal and LPS-induced IL-10 mRNA expressions were heightened in *Relb*$^{\Delta CD11c}$, but not *Nfkb2*$^{\Delta CD11c}$ BMDCs. Because of the shared colitis resilience phenotype of *Relb*$^{\Delta CD11c}$ and *Nkfb2*$^{\Delta CD11c}$ mice, we focused on Raldh2, whose expression was similarly affected upon ablation of either *Relb* or *Nfkb2* in BMDCs. We detected a 3.8-fold excess accumulation of Raldh2 protein in immunoblot analyses and a 2.2-fold increase in the basal Raldh enzymatic activity in aldefluor assay in *Relb*$^{\Delta CD11c}$ BMDCs (Figure 3G-3H). *Nfkb2*$^{\Delta CD11c}$ BMDCs revealed similar increases in the Raldh2 protein level and enzymatic activity (Figure S2F-2G). Previous studies involving DC-T cell co-culture established RA as an important determinant of LP DC-mediated conversion of naïve T cells into Tregs *ex vivo* (Sun et al., 2007). Our own analyses revealed that *Relb*$^{\Delta CD11c}$ BMDCs were more proficient in converting naïve splenic T cells into CD25$^+$Foxp3$^+$ CD4 Tregs *ex vivo*, and BMS493, a retinoic acid receptor (RAR) antagonist, erased this RelB-effect in DC-T cell co-culture (Figure 3I). Therefore, DC differentiation *ex vivo* appears to trigger constitutive activation of non-canonical NF-κB signaling, which suppresses the tolerogenic Raldh2-RA axis.

DC functions of the non-canonical NF-κB signal transducers limit the frequency of FoxP3$^+$ Treg in the mouse colon

Next, we examined immunoregulatory attributes of non-canonical NF-κB-deficient DCs *in vivo*. Deletion of *Relb* or *Nfkb2* in CD11c$^+$ cells did not significantly alter the frequency of DCs in MLNs or lamina propria (LP) in the colon (Figure 4A, Figure S3A). Also, when examined for the surface expression of CD80 and CD86 in flow cytometry

analyses, intestinal DCs from *Relb*$^{fl/fl}$ and *Relb*$^{\Delta CD11c}$ mice were indistinguishable (Figure 4B). Similarly, *Nfkb2*$^{fl/fl}$ and *Nfkb2*$^{\Delta CD11c}$ mice displayed equivalent levels of these co-stimulatory molecules on intestinal DCs (Figure S3B). Corroborating BMDCs studies, intestinal DCs from *Relb*$^{\Delta CD11c}$ mice, but not from *Nfkb2*$^{\Delta CD11c}$ mice, expressed significantly more IL-10 (Figure 4B-4C). However, RelB-dependent IL-10 regulation was more apparent in MLN DCs. Importantly, we could confirm an increased level of Raldh2 mRNA in intestinal DCs from both *Relb*$^{\Delta CD11c}$ and *Nfkb2*$^{\Delta CD11c}$ mice (Figure 4D). Our enzymatic assay substantiated a more than 2.1-fold rise in the Raldh activity in intestinal DCs from untreated *Relb*$^{\Delta CD11c}$ mice (Figure 4E). Thus, non-canonical NF-κB signaling regulated Raldh2 activity in DCs *in vivo*.

Raldh2 in intestinal DCs drives the synthesis of RA, which supports FoxP3 expressions and upregulates gut-homing receptors α4β7 and CCR9 in Tregs[28,29]. Indeed, the FoxP3$^+$ Treg frequency among CD4 T cells in LP and MLNs improved from 18.7% and 7.9% in *Relb*$^{fl/fl}$ mice to 36.6% and 12.4% in *Relb*$^{\Delta CD11c}$ mice, respectively (Figure 4F). While acute DSS treatment subtly skewed this Treg compartment at day 5, *Relb*$^{\Delta CD11c}$ mice maintained an overall increased level of these cells even in the colitogenic gut. Except for MLNs from untreated sets, the frequency of FoxP3$^+$ Tregs was similarly augmented in the intestine of *Nfkb2*$^{\Delta CD11c}$ mice (Figure 4G, Figure S3C). Notably, FoxP3$^+$ Tregs from MLNs of *Relb*$^{\Delta CD11c}$ mice were, if anything, subtly more efficient than those from *Relb*$^{fl/fl}$ counterparts in expressing IL-10 and α4β7, and displayed significantly elevated levels of CCR9 on their surface (Figure 4H). Inactivation of *Relb* or *Nfkb2* in CD11c$^+$ cells did not discernably alter the frequency of total CD4 T lymphocytes in the colon of untreated or DSS-treated mice (Figure S3D). Together, non-canonical NF-κB signaling impedes the Raldh2-mediated RA synthesis pathway in mucosal DCs, limiting the abundance of Tregs, and their gut-homing receptor expressions, in the intestine.

DC-intrinsic RelB function controls the abundance of IgA-secreting cells in the colon and gut microbiome

Previous studies suggested that RA promotes IgA-secreting cells at the gut mucosal interface[30]. We further explored whether reinforcing the RA pathway in non-canonical NF-κB-deficient DCs impacted intestinal sIgA levels. Our flow cytometry analyses disclosed a ~ 2.5-fold increase in the frequency of IgA$^+$B220$^+$ cells in LP of *Relb*$^{\Delta CD11c}$ mice (Figure 5A-5B), and our ELISA ascertained a significantly elevated fecal sIgA levels in this knockout (Figure 5C). Because sIgA coating is known to shape the gut microbiome[5,31], we performed 16s rRNA gene sequencing of fecal DNA to estimate the prevalence of different microbial taxa. We found that RelB deficiency was associated with changes specifically in two phyla; it led to an increase in the abundance of Firmicutes and a reduction in the level of Actinobacteriota in knockouts (Figure 5D). Another prominent phylum Bacteroidota showed a comparable fecal abundance among *Relb*$^{fl/fl}$ and *Relb*$^{\Delta CD11c}$ mice. Genus-level analyses of sequencing data similarly revealed gut microbiome alterations in these mice, including an expansion of *Sangeribacter* and *Lactobacillus* but also a reduction of *Akkermansia* and *Faecalibacterium* abundance (Figure 5E). Corroborating DNA sequencing studies, our qPCR analyses of fecal DNA substantiated changes in Firmicutes and Actinobacteriota in *Relb*$^{\Delta CD11c}$ mice (Figure 5F). Moreover, MACS-based fractionation of fecal pellet identified

enrichment of *Enterobacter*, *Bifidobacterium*, Segmented filamentous bacteria (SFB), *Sutterella* and *Prevotella* among IgA-bound gut microbes in *Relb*$^{\Delta CD11c}$ mice (Figure 5G). We also observed a decrease in the abundance of *β-proteobacteria* in the fecal IgA^{+} fraction in these knockouts.

Notably, Firmicutes, and more so the increased ratio of Firmicutes to Bacteroidota, have been linked to improved intestinal barrier integrity[32,33]. Likewise, *Sangeribacter*, *Lactobacillus*, and *Faecalibacterium* are thought to largely promote intestinal health[34]. Therefore, barring a reduction in *Faecalibacterium*, *Relb*$^{\Delta CD11c}$ mice had an overall preponderance of gut-beneficial taxa. More so, these changes were associated with differential sIgA coating of microbial entities. Importantly, differential sIgA-coating not only quantitatively impacts the microbiome composition but also qualitatively affects gene expressions and metabolic functions of microbial entities in the intestinal niche[5] . Curiously, *Nfkb2*$^{fl/fl}$ and *Nfkb2*$^{\Delta CD11c}$ mice were not discernibly different with respect to the frequency of intestinal IgA^{+}B220^{+} cells, luminal sIgA levels and the abundance of Firmicutes and Actinobacteriota (Figure 5B-5C, Figure 5F). Taken together, we deduce that a DC-intrinsic RelB function, where *Nfkb2* is dispensable, limits the accumulation of intestinal IgA^{+} B cells and luminal IgA, which likely foster a gut microbiome protective against experimental colitis in mice.

Non-canonical NF-κB signaling limits β-catenin-driven Raldh2 synthesis in DCs by directing Axin1 transcription

Previous studies identified Notch2, Irf4, and β-catenin as key factors directing the transcription of *Raldh2* in DCs[22,35,36]. We found that RelB depletion increased the abundance of specifically β-catenin, and not Notch2 or Irf4, in BMDCs (Figure 6A). Compared to respective controls, total β-catenin levels were elevated 4.2-fold in *Relb*$^{\Delta CD11c}$ and 3.6-fold in *Nfkb2*$^{\Delta CD11c}$ BMDCs (Figure 6B). This was accompanied by a proportionate increase in the level of active β-catenin and nuclear β-catenin in these knockouts. Importantly, pharmacological inhibition of β-catenin-mediated transcription in non-canonical NF-κB-deficient BMDCs using iCRT3 restored the Raldh2 protein abundance to that observed in control cells (Figure 6C). Therefore, our data supported a role of β-catenin in boosting Raldh2 production in the absence of non-canonical NF-κB signaling.

As such, Axin proteins tether β-catenin to a multiprotein destruction complex consisting of adenomatous polyposis coli (APC) and glycogen synthase kinase-3 (GSK-3) that promotes phosphorylation-dependent proteasomal degradation of β-catenin in resting cells[37] (Figure S4A). Wnt ligands signal through Frizzled receptors to rescue -catenin from this constitutive degradation. We argued that strengthening autocrine signaling owing to increased Wnt-secretion augmented β-catenin levels in knockouts. However, blocking the autocrine pathway with C59, a small molecule inhibitor of Wnt secretion from cells, did not discernibly change the abundance of β-catenin in *Relb*$^{\Delta CD11c}$ BMDCs (Figure 6D). We then investigated if non-canonical NF-κB deficiency instead impacted other β-catenin regulators. Examining our RNA-seq data indeed identified a significant decline in the mRNA level of the Axin1 isoform in *Nfkb2*$^{-/-}$ BMDCs (Figure 6E). When we analyzed the published RelB ChIP-seq dataset generated using WT BMDCs[38], the genome browser track of *Axin1* revealed

two distinct RelB peaks associated with a promoter and an intronic enhancer-κB element (Figure 6F). Our RT-qPCR studies substantiated that a dysfunctional non-canonical NF-κB pathway caused elevated expressions of Axin1 mRNA and protein in *Relb*$^{\Delta CD11c}$ and *Nfkb2*$^{\Delta CD11c}$ BMDCs (Figure 6G-6H). Notably, our immunoprecipitation experiments demonstrated that depleting Axin1 levels in *Relb*$^{\Delta CD11c}$ BMDCs impeded the association of β-catenin with GSK3β, a critical component of the destruction complex (Figure 6I). We conclude that non-canonical NF-κB-mediated transcriptional control of Axin1 suppresses β-catenin-driven Raldh2 expressions in DCs.

β-catenin determines immunoregulatory DC functions of the non-canonical NF-κB pathway in the intestine

Previous studies suggested that DC-intrinsic functions of β-catenin limits mucosal inflammation in the intestine[22,39]. Corroborating our *ex vivo* analyses, we observed an increased abundance of β-catenin in intestinal DCs from *Relb*$^{\Delta CD11c}$ or *Nfkb2*$^{\Delta CD11c}$ mice compared to those from respective control floxed mice (Figure 7A, Figure S4B). To causally establish if β-catenin accumulation in non-canonical NF-κB-deficient DCs alleviated colitogenic pathologies, we introduced a DC-specific β-catenin haploinsufficiency in mice devoid of RelB expression in DCs. Convincingly, MLN DCs from *Ctnnb1*$^{fl/+}$*Relb*$^{\Delta CD11c}$ mice displayed a significant drop in the Raldh2 activity from those in *Relb*$^{\Delta CD11c}$ mice (Figure 7B). Consistent with the tolerogenic role of DC-expressed Raldh2, the levels of colonic FoxP3^{+} Tregs and fecal sIgA in *Ctnnb1*$^{fl/+}$*Relb*$^{\Delta CD11c}$ mice were restored to those in *Relb*$^{fl/fl}$ mice (Figure 7C-7D). When challenged in the acute regime, *Ctnnb1*$^{fl/+}$*Relb*$^{\Delta CD11c}$ mice exhibited bodyweight loss and colon shortening at day 6, which were rather analogous to *Relb*$^{fl/fl}$ mice (Figure 7E-7F). Previous studies linked IBD to decreased Raldh activity in intestinal DCs[6]. The available single-cell RNA-seq data[23] revealed little or no expressions of several *bona fide* β-catenin targets in intestinal DCs from IBD patients. However, we could demonstrate that *CCND1*, a gene known to be activated by β-catenin, were expressed by approximately 20% of intestinal DCs and substantially downmodulated in human IBD (Figure 7G). Collectively, our investigation advocates that the non-canonical NF-κB pathway targets β-catenin to limit the tolerogenic Raldh2 functions in intestinal DCs, leading to a reduction in Tregs and sIgA in the colitogenic gut (Figure 7H).

Discussion

Despite the known role of the non-canonical NF-κB pathway in DCs in mounting protective as well as pathogenic T cell responses[16–18,20], if DC-intrinsic RelB:p52 functions modulate inflammatory pathologies in the intestine remains unclear. Our investigation identified strengthening non-canonical NF-κB signaling in intestinal DCs from IBD patients and causally linked this pathway to exacerbated colitis in mice (Figure 1-2). DC-derived RA imparts tolerogenic attributes, and β-catenin induces the expression of the RA-synthesizing enzyme Raldh2 in intestinal DCs[22,28,40,41]. Our mechanistic studies suggested that RelB:p52

transcriptionally supported Axin1, which restrained Raldh2 synthesis in DCs by downmodulating β-catenin (Figure 3, Figure 6). Concordantly, non-canonical NF-κB impairment reinforced β-catenin-mediated Raldh2 expressions in DCs, improving the colonic frequency of protective Tregs and luminal sIgA levels, which were associated with a modified gut microbiome (Figure 4-5). Indeed, introducing β-catenin haploinsufficiency in RelB-deficient DCs reinstated the colitogenic sensitivity in mice (Figure 7). IBD is multifactorial, and DC dysfunctions aggravate the disease pathogenesis. Here, we elucidate the role of non-canonical NF-κB signaling in instructing immunoregulatory DC functions in the gut through negative control of the RA synthesis pathway (Figure 7H).

It was earlier reported that DC-specific ablation of *Relb*, but not *Nfkb2*, led to a systemic increase in the frequency of FoxP3$^+$ Tregs[19]. We found a convergence of *Relb*$^{\Delta CD11c}$ and *Nfkb2*$^{\Delta CD11c}$ mice with respect to immune phenotypes – they both accumulated FoxP3$^+$ Tregs in the intestine and were resilient to experimental colitis. Our data contended that systemic Treg effects were less important and that β-catenin-dependent modulation of specifically the intestinal Treg compartment was critical for the colitogenic role of RelB:p52 in DCs. As opposed to a substantial increase in the intestinal Treg frequency in *Relb*$^{\Delta CD11c}$ mice, RelB-depleted DCs *ex vivo* displayed only modest, albeit RA pathway-dependent, enhancement of Treg generation from naïve T cells. Based on the literature[29] and our study, we reason that in addition to its role in priming Treg differentiation, DC-derived RA also promoted gut homing of Tregs and their stabilization in the intestinal niche in the knockout mice. Additionally, RelB in DCs was shown to promote microbiota-reactive RORγt+ Tregs in the small intestine[19]. Although our study did not distinguish between tissue- and microbiota-reactive Tregs in the colon, we speculate that the observed increase in the frequency of FoxP3$^+$ Tregs in our knockouts could be driven by tissue Tregs. Importantly, other than microbiota-reactive Tregs, tissue Tregs were also found to be critical for tolerance to gut commensals[42]. Of note, it was suggested that NIK in DCs induced the expression of IL-23, which strengthened Th17 responses to *Citrobacter rodentium*[20]. A similar DC-intrinsic role of RelB in promoting IL-23-mediated Th17 response to gut commensals cannot be ruled out. However, our work argues that Th17 regulations by RelB in DC could be secondary non-canonical NF-κB-mediated Treg controls, at least in the intestinal niche.

We further noticed interesting differences between *Relb* and *Nfkb2* genotypes. In particular, *Nfkb2*-deficient DCs did not show elevated IL-10 expressions as observed in RelB-deficient DCs. *Relb*$^{\Delta CD11c}$ mice accumulated intestinal IgA$^+$ B cells, whereas *Nfkb2*$^{\Delta CD11c}$ mice did not. Unlike *Relb*$^{\Delta CD11c}$ mice, *Nfkb2*$^{\Delta CD11c}$ mice did not readily produce a phenotype in the DSS-induced acute colitis regime (Figure S1G). Previous studies suggested that IL-10, in addition to DC-derived RA, promotes IgA class switch in the gut[2], and also documented an inhibitory role of RelB in DC-mediated IL-10 expressions[43]. Additionally, RelB:p50 heterodimer was shown to partially compensate for the lack of RelB:p52 in the *Nfkb2*-deficient cell system[25]. In light of these studies, we conjecture that RelB:p50 and RelB:p52 acted redundantly in DCs in downmodulating IL-10, while a non-redundant role of RelB:p52 in Axin1 transcription restrained β-catenin-dependent Raldh2 synthesis. Accordingly, ablating *Relb* in DCs supported the synergy between IL-10 and the RA pathway, culminating in the increased luminal IgA level. Conversely, RelB:p50 may have

masked the phenotype of *Nfkb2*$^{\Delta CD11c}$ mice in the acute regime by preventing heightened IL-10 expressions in knockout DCs and, thereby, changes in the intestinal IgA^{+} cell compartment. *Nfkb2*$^{\Delta CD11c}$ mice also displayed a somewhat less marked increase in the frequency of intestinal Tregs compared to *Relb*$^{\Delta CD11c}$ mice, presumably owing to IL-10 expression differences between these genotypes. While the biochemical mechanism underlying RelB-mediated IL-10 control warrants further investigation, our comparison involving *Relb*$^{\Delta CD11c}$ and *Nfkb2*$^{\Delta CD11c}$ strains identified distinct as well as overlapping gene controls by the non-canonical NF-κB signal transducers *Relb* and *Nfkb2* in DCs with implications for intestinal health.

The widely known role of the non-canonical NF-κB pathway lies in lymphoid stromal cells in supporting the expression of homeostatic lymphokines, which promote secondary lymph node development during early embryogenesis and also lymphocyte ingress in lymph nodes in adults[15,44]. In addition, an *Nfkb2*-dependent cross regulatory mechanism was shown to aggravate colon inflammation by escalating RelA-driven inflammatory gene expressions in IECs[24]. Our work unequivocally established that non-canonical RelB:p52 NF-κB signaling in DCs inhibited the tolerogenic β-catenin-Raldh2 axis, fueling intestinal pathologies. Beyond tolerogenic DC functions, β-catenin and the Raldh2-RA pathway have other biological roles. For example, β-catenin deregulations in intestinal epithelial cells drive colon cancer[45]. In a recent study, Conlon et al (2020) suggested that LTβR inhibits WNT/β-catenin signaling in lung epithelial cells, exacerbating tissue damage in chronic obstructive pulmonary disease[46]. On the other hand, neuronal-derived RA promoted early lymph node biogenesis[47], and intestinal DC-secreted RA was critical for the maintenance of secondary lymph nodes[48]. We argue that our work may provide for a significant revision of our understanding of non-canonical NF-κB functions in physiology and disease. To this end, future studies ought to examine the potential trigger of non-canonical NF-κB signaling in various anatomic niches and their plausible impact on β-catenin activity or the RA pathway in shaping immune responses or developmental processes.

Finally, micronutrients are emerging as important determinants of mucosal immunity and potential interventional tools for inflammatory ailments[49]. Previous studies indicated that vitamin D exerts a negative impact on RelB synthesis in DCs [50,51]. As such, Raldh2 empowers intestinal DCs to secrete constitutively copious amounts of RA. Our current investigation posits that non-canonical NF-κB signaling curbs this immunomodulatory retinoic acid synthesis pathway in intestinal DCs, imparting vulnerability to colitogenic insults. Therefore, it appears that beyond its well-articulated role in immune gene expressions, DC-intrinsic non-canonical NF-κB signaling could be also critical for the micronutrient control of intestinal inflammation. While the significance of our study in the context of nutritional or DC-based therapy remains to be tested, we, in sum, establish a DC network integrating immune signaling and micronutrient metabolic pathways in the intestine.

Materials and Methods

See Supplementary file.

Data and Software Availability

The MIAME version of the RNA seq dataset is available on NCBI Gene Expression Omnibus accession GSE249101, and the microbiome data is available at the accession PRJNA1046443.

Supplemental Information

Supplemental Information consists of material/methods and four supplementary figures.

Acknowledgement

We thank Prof. Amitabha Bandyopadhyay, IIT Kanpur for help with *Ctnnb*$^{fl/fl}$ mice. We thank V. Kumar for technical support and Dr. P. Nagarajan for the help with animal husbandry. Research in the PI's laboratory was funded by DBT (BT/PR36631/BRB/10/1862/2020) and NII-Core. AD and NK thank DST-INSPIRE and DBT, respectively, for research fellowships.

Author Contribution

A.D., N.K. and S.B. conceptualized the study and analyzed data. A.D. and N.K. performed the experiments with help from M.C., S.A.A., and B.C. Flow cytometry analyses were carried out with help from U.M. and guidance from A.A. 16s rRNA sequencing and data analyses were done with help from S.K. and supervision from B.D. Single-cell transcriptomics data was analyzed by N. K. and N.B. with guidance from D.S. ChIP-seq data analyses was performed by Sw.B. A.D., N.K. and S.B. wrote the manuscript.

Declaration of Interests

The authors declare no conflict of interest.

Figure Legend

Figure 1: Charting non-canonical NF-κB signaling in intestinal DCs from IBD patients and colitogenic mice

- **A.** UMAP comparing IBD patients and non-IBD subjects for the level of *RELB* and *NFKB2* mRNAs in intestinal DCs. Single-cell RNA-seq data available at the Single Cell Portal was used for analyses (SCP259). 1819 DCs were examined; the intensity of dot color denotes the abundance of corresponding mRNAs in each cell.
- **B.** and **C.** Dot plot revealing the expression of indicated genes in intestinal DCs from IBD patients and control subjects. The color gradient of dots represents the average expression level, while the dot size denotes the percentage of cells expressing a given gene.
- **D.** UMAP depicting the expression of *Relb* and *Nfkb2* mRNAs in a time course in intestinal DCs from WT mice subjected to DSS-induced acute colitis. Single-cell RNA-seq data available at the NCBI database was used for analyses (GSE148794).
- **E.** and **F.** Dot plot revealing quantified levels of indicated mRNAs in intestinal DCs from the WT mice left untreated or subjected to DSS treatment.
- **G.** Boxplot (left) showing the abundance of p52 in relation to p100 in intestinal DCs determined by quantifying the respective band intensities in immunoblot analyses (right). DCs were collected from MLNs of untreated mice or those administered with 2% DSS in drinking water for 5 days.

Data represents mean ± SEM. For statistical analyses, two-tailed Student's t-test was performed.

Figure 2: Ablating non-canonical NF-κB functions in CD11c^{+} cells ameliorate experimental colitis in mice

- **A.** and **B.** *Relb*$^{fl/fl}$ and *Relb*$^{\Delta CD11c}$ mice were subjected to acute DSS treatment for 7 days and changes in the bodyweight **(A)** and colon length **(B)** were monitored. Representative colon images have been shown next to the dot plot **(B)**.
- **C.** Representative images of H&E-stained colon sections from the indicated mice left untreated or subjected to acute DSS treatment. The data represent n = 5; 4 fields per section and a total of 5 sections from each set were examined. Black arrows indicate edema, leucocyte infiltration and epithelial lining damage. Scale bar, 50µm.
- **D.** Scatter plot revealing the serum concentration of FITC-dextran in *Relb*$^{fl/fl}$ and *Relb*$^{\Delta CD11c}$ mice left untreated or subjected to acute DSS treatment; FITC-dextran was gavaged orally 6h prior to serum collection.
- **E.** RT-qPCR demonstrating the colonic abundance of indicated mRNAs in untreated or DSS-treated *Relb*$^{fl/fl}$ and *Relb*$^{\Delta CD11c}$ mice.
- **F.** and **G.** In a chronic colitis regime, *Nfkb2*$^{fl/fl}$ and *Nfkb2*$^{\Delta CD11c}$ mice were subjected to 3 cycles of DSS treatment, where each cycle involved 7 days of 1% DSS treatment followed by 14 days of recovery. Subsequently, changes in the bodyweight **(F)** and colon length **(G)** were measured.

Data represents mean ± SEM. Two-tailed Student's t-test was performed. *P < 0.05; **P < 0.01; ***P < 0.001; ns, not significant.

Figure 3: Defective *Relb* or *Nfkb2* functions enhance the expression and activity of Raldh2 in DCs

- **A.** Immunoblot charting the abundance of p52 and p100 in whole cell extracts (top) or RelB and p52 in nuclear extracts (bottom) in cells harvested from BMDC-differentiating culture at the indicated days.
- **B.** Enrichment analyses revealing top 10 enriched DC-relevant biological pathways among genes differentially expressed between *Nfkb2*$^{-/-}$ and WT BMDCs. For each genotype, RNA-seq data from three independent biological replicates were used.
- **C.** GSEA comparing *Nfkb2*$^{-/-}$ and WT BMDCs for the enrichment of RA targets among differentially expressed genes (top). Fold change (FC) in the basal mRNA level between these genotypes was considered to create a ranked gene list, which was subjected to GSEA. Vertical lines represent individual RA targets. ES and NES denote enrichment and normalized enrichment scores, respectively.
- **D.** A cartoon describing the RA metabolism pathway and its functions in DCs.
- **E.** Heatmap showing the expression of selected RA metabolism-associated genes in WT and *Nfkb2*$^{-/-}$ BMDCs, as determined in RNA-seq.
- **F.** RT-qPCR comparing untreated or LPS-treated BMDCs derived from *Relb*$^{fl/fl}$ and *Relb*$^{\Delta CD11c}$ mice (left) or *Nfkb2*$^{fl/fl}$ and *Nfkb2*$^{\Delta CD11c}$ mice (right) for gene expressions.
- **G.** Representative immunoblot revealing the abundance of Raldh2 in *Relb*$^{fl/fl}$ and *Relb*$^{\Delta CD11c}$ BMDCs. Corresponding band intensities were quantified and presented as a barplot below.
- **H.** Histograms showing the Raldh enzymatic activity measured by Aldefluor assay in BMDCs. The Raldh inhibitor DEAB was used as a control. For a given genotype, ΔMFI was calculated as = $MFI_{no\ DEAB}$ - MFI_{DEAB}, and presented in a barplot.
- **I.** Flow cytometry analyses demonstrating the generation of $CD25^{+}Foxp3^{+}$ CD4 Treg in DC-T cell co-culture *ex vivo*. Briefly, BMDCs were cultured with naïve T cells, isolated from the spleen of WT mice, in the presence of CD3 and TGF-β for 3.5 days. In specified sets, the RAR inhibitor BMS493 was added. The frequency of $CD25^{+}Foxp3^{+}$ Treg as a percentage of CD4 cells was determined and presented in the barplot (bottom).

Data represent mean ± SEM. Two-tailed Student's t-test was performed. *P < 0.05; **P < 0.01; ns, not significant.

Figure 4: Disruption of non-canonical NF-κB signaling in $CD11c^{+}$ cells accumulates $FoxP3^{+}$ Treg in the mouse colon

- **A.** Flow cytometry studies indicating the abundance of DCs, as a percentage of CD45+ cells, in MLN or LP.
- **B.** Representative histograms showing the expression of CD80, CD86 and IL-10 in DCs from LP or MLN from *Relb*$^{fl/fl}$ and *Relb*$^{\Delta CD11c}$ mice.
- **C.** Barplot revealing MFI for IL-10 expression in MLN DCs from the indicated mice.

D. RT-qPCR depicting the abundance of Raldh2 mRNA in MLN DCs from *Relb*$^{fl/fl}$ and *Relb*$^{\Delta CD11c}$ or *Nfkb2*$^{fl/fl}$ and *Nfkb2*$^{\Delta CD11c}$ mice.

E. Histograms capturing Raldh enzymatic activity in MLN DCs from *Relb*$^{fl/fl}$ and *Relb*$^{\Delta CD11c}$ mice. Quantified average MFI has been presented in a barplot.

F. Representative contours from flow cytometry analyses showing the frequency of Foxp3^{+} Tregs as a percentage of CD4^{+} T cells in LP or MLNs of untreated or DSS-treated *Relb*$^{fl/fl}$ and *Relb*$^{\Delta CD11c}$ mice. Corresponding quantified data has been presented as a barplot in the right.

G. Barplot revealing the mean frequency of Foxp3^{+} Treg in LP and MLN of *Nfkb2*$^{fl/fl}$ and *Nfkb2*$^{\Delta CD11c}$ mice.

H. Overlapping histograms depicting the expression of IL-10, α4β7 and CCR9 in Foxp3^{+} Tregs from MLNs of *Relb*$^{fl/fl}$ and *Relb*$^{\Delta CD11c}$ mice. Quantified average MFIs are indicated in the individual barplot below.

Each datapoint signifies an individual mouse; data represent mean ± SEM. Two-tailed Student's t-test was performed. *P < 0.05; **P < 0.01; ***P < 0.001; ns, not significant.

Figure 5: RelB-NF-κB deficiency in CD11c^{+} cells as a determinant of the intestinal abundance of IgA-secreting cells and gut microbiome

A. Representative FACS plots revealing the frequency of IgA^{+}B220^{+} cells as a percentage of CD19^{+} cells in LP of *Relb*$^{fl/fl}$ and *Relb*$^{\Delta CD11c}$ mice.

B. Barplot demonstrating quantified frequency of IgA^{+} B220^{+} cells in LP of mice of the indicated genotypes.

C. ELISA comparing *Relb*$^{fl/fl}$ and *Relb*$^{\Delta CD11c}$ mice for sIgA concentrations in fecal pellets.

D. and **E.** The relative abundance of various microbial phyla **(D)** and genera **(E)** charted in barplot **(D)** and heatmap **(E)**, respectively. Briefly, 16s rDNA sequencing was performed using fecal DNA from *Relb*$^{fl/fl}$ and *Relb*$^{\Delta CD11c}$ mice and prevalent phyla and genera were plotted.

F. 16s rDNA-based qPCR analyses of fecal DNA showing the level of indicated microbial taxa in *Relb*$^{fl/fl}$ and *Relb*$^{\Delta CD11c}$ or *Nfkb2*$^{fl/fl}$ and *Nfkb2*$^{\Delta CD11c}$ mice.

G. qPCR analyses MACS-sorted IgA^{+} fractions of fecal pellets comparing *Relb*$^{fl/fl}$ and *Relb*$^{\Delta CD11c}$ mice for the prevalence of the indicated bacteria.

Each datapoint represents an individual mouse; data represent mean ± SEM. Two-tailed Student's t-test was performed for Figure 5A-5C and one-way ANOVA was carried out for Figure 5F-5G. *P < 0.05; **P < 0.01; ns, not significant.

Figure 6: Reduced transcription of Axin1 promotes β-catenin-driven Raldh2 synthesis in noncanonical NF-κB-deficient DCs

A. Immunoblot analyses comparing *Relb*$^{fl/fl}$ and *Relb*$^{\Delta CD11c}$ BMDCs for the abundance of the indicated transcription factors.

B. Representative immunoblot revealing active and total β-catenin levels in whole-cell or nuclear extracts derived from BMDCs of the indicated genotypes. Total β-catenin band intensities were also quantified and presented as barplot (right). Gapdh and Tbp served as loading controls for whole-cell and nuclear extracts, respectively.

C. Immunoblot charting Raldh2 mRNA level in *Relb*$^{fl/fl}$ and *Relb*$^{\Delta CD11c}$ BMDCs left untreated or treated with 50μM of iCRT3, which inhibits β-catenin-mediated transcription, for 12h.

D. Immunoblot analyses capturing the abundance of β-catenin in *Relb*$^{\Delta CD11c}$ BMDCs treated for 24h with 10μM of C59, which prevents secretion of Wnt ligands by inhibiting Porcupine.

E. Heatmap comparing the abundance of mRNAs encoding the indicated β-catenin regulators in WT and *Nfkb2*$^{-/-}$ BMDCs, as determined by RNA-seq.

F. The genome browser track of RelB ChIP-seq peaks in WT BMDCs (GSE236531) for *Axin1*. Cognate κB motifs associated with these peaks have also been indicated.

G. and **H.** RT-qPCR **(G)** and immunoblot **(H)** analyses scoring the level of Axin1 mRNA **(G)** and protein **(H)**, respectively, in BMDCs. For immunoblot analyses, corresponding band intensities were quantified and presented (bottom).

I. Immunoblot analyses of β-catenin co-immunoprecipitates obtained using *Relb*$^{fl/fl}$ and *Relb*$^{\Delta CD11c}$ BMDCs subjected to MG-132 treatment for 4h. Left, MG-132-treated cell extracts used as inputs for immunoprecipitation. MG-132 treatment was carried out to achieve comparable β-catenin levels between WT and knockout BMDCs. # represents non-specific bands.

Quantified data represent the mean of at least three experimental replicates ± SEM. Two-tailed Student's t-test was performed. *P < 0.05; **P < 0.01.

Figure 7: Haploinsufficiency of β-catenin in non-canonical NF-κB deficient DCs reinstates the colitogenic phenotype in mice

A. Histograms comparing *Relb*$^{fl/fl}$ and *Relb*$^{\Delta CD11c}$ mice for the expression of β-catenin in MLN DCs. Quantified MFI for -catenin has also been presented in a barplot.

B. Histograms revealing the Raldh activity in MLN DCs from *Relb*$^{fl/fl}$, *Relb*$^{\Delta CD11c}$ and *Ctnnb1*^{hetCD11c}*Relb*$^{\Delta CD11c}$ mice. Corresponding ΔMFI values calculated from corresponding DEAB controls have been presented in the barplot.

C. Barplot revealing the mean frequency of Foxp3^{+} Tregs in LP of indicated mice.

D. ELISA comparing fecal IgA levels of the indicated genotypes.

E. and **F.** Scatter plots revealing colon length and bodyweight changes on the day 6 upon acute DSS treatment of indicated mice.

G. Dot plot revealing the expression of indicated β-catenin target genes in intestinal DCs from IBD patients and control subjects. The data was derived from published single-cell RNA-seq data (Ref: SCP259).

H. A cartoon depicting a noncanonical NF-κB pathway-driven signaling circuitry in DCs that tunes intestinal inflammation.

Each datapoint represents an individual mouse; data represent mean ± SEM. For statistical tests, One-way ANOVA was performed. **P < 0.01; ***P < 0.001; ns, not significant.

References

1. Stagg, A. J. Intestinal Dendritic Cells in Health and Gut Inflammation. *Frontiers in Immunology* vol. 9 Preprint at https://doi.org/10.3389/fimmu.2018.02883 (2018).
2. Xu, W. *et al.* Epithelial cells trigger frontline immunoglobulin class switching through a pathway regulated by the inhibitor SLPI. *Nat Immunol* **8**, (2007).
3. Seo, G.-Y. *et al.* Retinoic acid, acting as a highly specific IgA isotype switch factor, cooperates with TGF-β1 to enhance the overall IgA response. *J Leukoc Biol* **94**, (2013).
4. Bunker, J. J. *et al.* Natural polyreactive IgA antibodies coat the intestinal microbiota. *Science (1979)* **358**, (2017).
5. Nakajima, A. *et al.* IgA regulates the composition and metabolic function of gut microbiota by promoting symbiosis between bacteria. *Journal of Experimental Medicine* **215**, (2018).
6. Magnusson, M. K. *et al.* Macrophage and dendritic cell subsets in IBD: ALDH+ cells are reduced in colon tissue of patients with ulcerative colitis regardless of inflammation. *Mucosal Immunol* **9**, (2016).
7. Collins, C. B. *et al.* Retinoic acid attenuates ileitis by restoring the balance between T-helper 17 and t regulatory cells. *Gastroenterology* **141**, (2011).
8. Manoharan, I. *et al.* The Transcription Factor RXRα in CD11c+ APCs Regulates Intestinal Immune Homeostasis and Inflammation. *The Journal of Immunology* **211**, (2023).
9. Jin, J. *et al.* CD137 Signaling Regulates Acute Colitis via RALDH2-Expressing CD11b−CD103+ DCs. *Cell Rep* **30**, (2020).
10. Okayasu, I. *et al.* Vitamin A Inhibits Development of Dextran Sulfate Sodium-Induced Colitis and Colon Cancer in a Mouse Model. *Biomed Res Int* **2016**, (2016).
11. Kau, A. L. *et al.* Functional characterization of IgA-targeted bacterial taxa from undernourished Malawian children that produce diet-dependent enteropathy. *Sci Transl Med* **7**, (2015).
12. Palm, N. W. *et al.* Immunoglobulin A coating identifies colitogenic bacteria in inflammatory bowel disease. *Cell* **158**, (2014).
13. Liu, T., Zhang, L., Joo, D. & Sun, S. C. NF-κB signaling in inflammation. *Signal Transduction and Targeted Therapy* vol. 2 Preprint at https://doi.org/10.1038/sigtrans.2017.23 (2017).
14. Visekruna, A. *et al.* Transcription factor c-Rel plays a crucial role in driving anti-CD40-mediated innate colitis. *Mucosal Immunol* **8**, (2015).
15. Sun, S. C. The non-canonical NF-κB pathway in immunity and inflammation. *Nature Reviews Immunology* vol. 17 Preprint at https://doi.org/10.1038/nri.2017.52 (2017).
16. Shih, V. F. S. *et al.* Control of RelB during dendritic cell activation integrates canonical and noncanonical NF-κB pathways. *Nat Immunol* **13**, (2012).
17. Hofmann, J., Mair, F., Greter, M., Schmidt-Supprian, M. & Becher, B. NIK signaling in dendritic cells but not in T cells is required for the development of effector T cells and cell-mediated immune responses. *Journal of Experimental Medicine* **208**, (2011).
18. Huang, T. *et al.* CRL4DCAF2 negatively regulates IL-23 production in dendritic cells and limits the development of psoriasis. *Journal of Experimental Medicine* **215**, 1999–2017 (2018).

19. Andreas, N. *et al.* RelB Deficiency in Dendritic Cells Protects from Autoimmune Inflammation Due to Spontaneous Accumulation of Tissue T Regulatory Cells. *The Journal of Immunology* **203**, (2019).
20. Jie, Z. *et al.* NIK signaling axis regulates dendritic cell function in intestinal immunity and homeostasis. *Nat Immunol* **19**, (2018).
21. Liu, J. Z. *et al.* Association analyses identify 38 susceptibility loci for inflammatory bowel disease and highlight shared genetic risk across populations. *Nat Genet* **47**, (2015).
22. Manicassamy, S. *et al.* Activation of β-catenin in dendritic cells regulates immunity versus tolerance in the intestine. *Science (1979)* **329**, (2010).
23. Smillie, C. S. *et al.* Intra- and Inter-cellular Rewiring of the Human Colon during Ulcerative Colitis. *Cell* **178**, (2019).
24. Chawla, M. *et al.* An epithelial Nfkb2 pathway exacerbates intestinal inflammation by supplementing latent RelA dimers to the canonical NF-κB module. *Proc Natl Acad Sci U S A* **118**, (2021).
25. Basak, S., Shih, V. F.-S. & Hoffmann, A. Generation and Activation of Multiple Dimeric Transcription Factors within the NF-κB Signaling System. *Mol Cell Biol* **28**, (2008).
26. Wirtz, S. *et al.* Chemically induced mouse models of acute and chronic intestinal inflammation. *Nat Protoc* **12**, (2017).
27. Kedishvili, N. Y. Retinoic acid synthesis and degradation. *Subcell Biochem* **81**, (2016).
28. Iwata, M. *et al.* Retinoic acid imprints gut-homing specificity on T cells. *Immunity* **21**, (2004).
29. Lu, L. *et al.* Critical role of all-trans retinoic acid in stabilizing human natural regulatory T cells under inflammatory conditions. *Proc Natl Acad Sci U S A* **111**, (2014).
30. Villablanca, E. J. *et al.* MyD88 and retinoic acid signaling pathways interact to modulate gastrointestinal activities of dendritic cells. *Gastroenterology* **141**, (2011).
31. Pabst, O. & Izcue, A. Secretory IgA: controlling the gut microbiota. *Nat Rev Gastroenterol Hepatol* **19**, (2022).
32. Stojanov, S., Berlec, A. & Štrukelj, B. The influence of probiotics on the firmicutes/bacteroidetes ratio in the treatment of obesity and inflammatory bowel disease. *Microorganisms* vol. 8 Preprint at https://doi.org/10.3390/microorganisms8111715 (2020).
33. Sun, Y. *et al.* Gut firmicutes: Relationship with dietary fiber and role in host homeostasis. *Critical Reviews in Food Science and Nutrition* Preprint at https://doi.org/10.1080/10408398.2022.2098249 (2022).
34. Forster, S. C. *et al.* Identification of gut microbial species linked with disease variability in a widely used mouse model of colitis. *Nat Microbiol* **7**, (2022).
35. Yashiro, T., Yamaguchi, M., Watanuki, Y., Kasakura, K. & Nishiyama, C. The Transcription Factors PU.1 and IRF4 Determine Dendritic Cell–Specific Expression of RALDH2. *The Journal of Immunology* **201**, (2018).
36. Zaman, T. S. *et al.* Notch Balances Th17 and Induced Regulatory T Cell Functions in Dendritic Cells by Regulating Aldh1a2 Expression . *The Journal of Immunology* **199**, (2017).

37. MacDonald, B. T., Tamai, K. & He, X. Wnt/β-Catenin Signaling: Components, Mechanisms, and Diseases. *Developmental Cell* vol. 17 Preprint at https://doi.org/10.1016/j.devcel.2009.06.016 (2009).
38. Navarro, H. I. *et al.* RelB-deficient autoinflammatory pathology presents as interferonopathy, but in mice is interferon-independent. *Journal of Allergy and Clinical Immunology* **152**, (2023).
39. Zhao, F. *et al.* Paracrine Wnt5a-β-Catenin Signaling Triggers a Metabolic Program that Drives Dendritic Cell Tolerization. *Immunity* **48**, (2018).
40. Bos, A., van Egmond, M. & Mebius, R. The role of retinoic acid in the production of immunoglobulin A. *Mucosal Immunology* vol. 15 Preprint at https://doi.org/10.1038/s41385-022-00509-8 (2022).
41. Coombes, J. L. *et al.* A functionally specialized population of mucosal CD103+ DCs induces Foxp3+ regulatory T cells via a TGF-β -and retinoic acid-dependent mechanism. *Journal of Experimental Medicine* **204**, (2007).
42. Cebula, A. *et al.* Thymus-derived regulatory T cells contribute to tolerance to commensal microbiota. *Nature* **497**, (2013).
43. Duan, J. L. *et al.* E3 ligase c-Cbl regulates intestinal inflammation through suppressing fungi-induced noncanonical NF-κB activation. *Sci Adv* **7**, (2021).
44. Mukherjee, T. *et al.* A TNF -p100 pathway subverts noncanonical NF -κB signaling in inflamed secondary lymphoid organs . *EMBO J* **36**, (2017).
45. Zhao, H. *et al.* Wnt signaling in colorectal cancer: pathogenic role and therapeutic target. *Molecular Cancer* vol. 21 Preprint at https://doi.org/10.1186/s12943-022-01616-7 (2022).
46. Conlon, T. M. *et al.* Publisher Correction: Inhibition of LTβR signalling activates WNT-induced regeneration in lung (Nature, (2020), 588, 7836, (151-156), 10.1038/s41586-020-2882-8). *Nature* vol. 589 Preprint at https://doi.org/10.1038/s41586-020-03087-6 (2021).
47. Van De Pavert, S. A. *et al.* Chemokine cxcl13 is essential for lymph node initiation and is induced by retinoic acid and neuronal stimulation. *Nat Immunol* **10**, (2009).
48. Zhang, Z. *et al.* Peripheral Lymphoid Volume Expansion and Maintenance Are Controlled by Gut Microbiota via RALDH+ Dendritic Cells. *Immunity* **44**, (2016).
49. Gombart, A. F., Pierre, A. & Maggini, S. A review of micronutrients and the immune system–working in harmony to reduce the risk of infection. *Nutrients* **12**, (2020).
50. Ratra, Y. *et al.* A Vitamin D–RelB/NF-κB Pathway Limits Chandipura Virus Multiplication by Rewiring the Homeostatic State of Autoregulatory Type 1 IFN–IRF7 Signaling. *The Journal of Immunology* **209**, (2022).
51. Dong, X. *et al.* Regulation of relB in dendritic cells by means of modulated association of vitamin D receptor and histone deacetylase 3 with the promoter. *Proc Natl Acad Sci U S A* **102**, (2005).

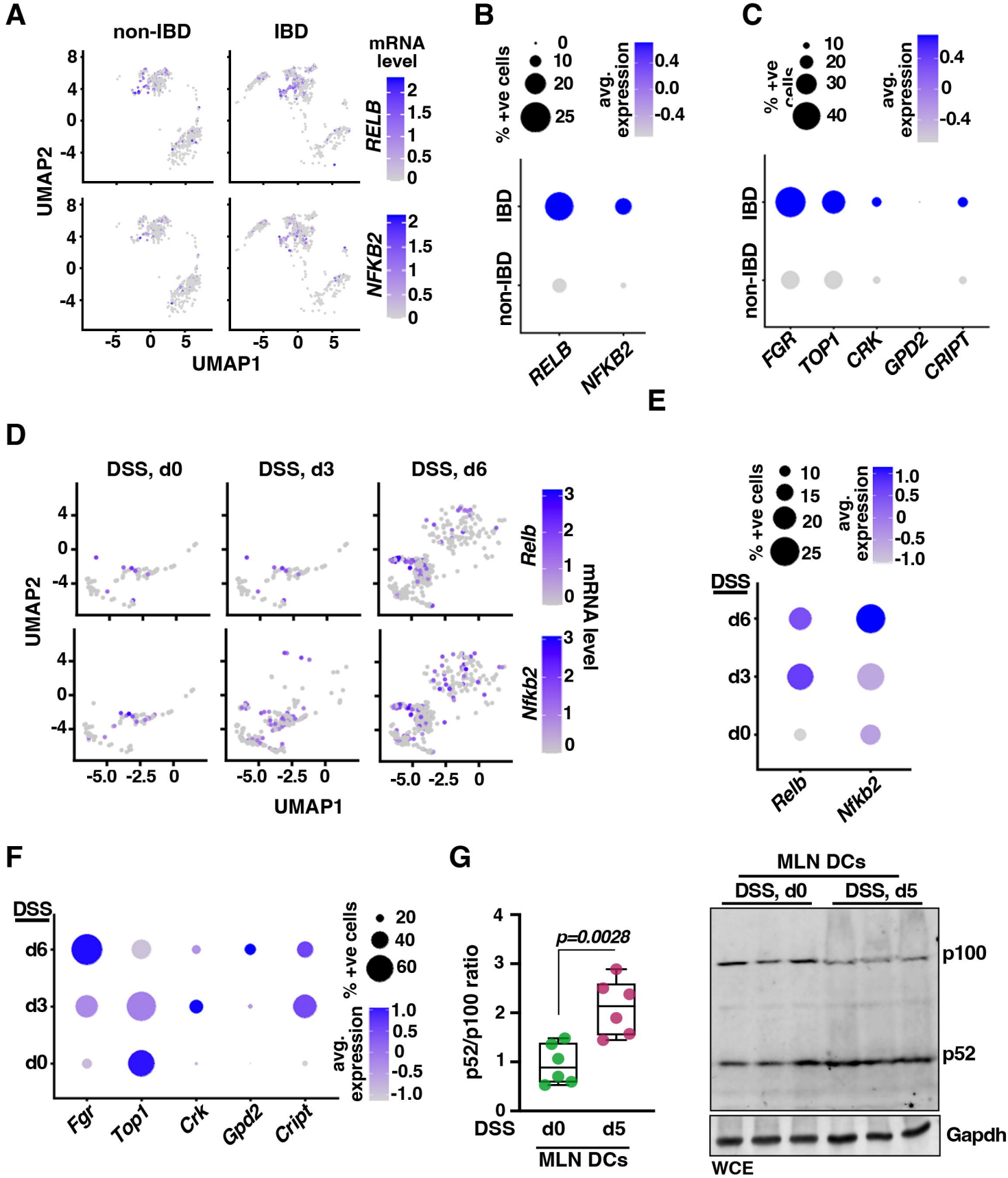
A
non-IBD
IBD
mRNA level
RELB
NFKB2
UMAP2
UMAP1
B
% +ve cells
avg. expression
IBD
non-IBD
RELB
NFKB2
C
IBD
non-IBD
FGR
TOP1
CRK
GPD2
CRIPT
D
DSS, d0
DSS, d3
DSS, d6
Relb
Nfkb2
mRNA level
UMAP2
UMAP1
E
% +ve cells
avg. expression
DSS
d6
d3
d0
Relb
Nfkb2
F
DSS
d6
d3
d0
Fgr
Top1
Crk
Gpd2
Cript
% +ve cells
avg. expression
G
p52/p100 ratio
p=0.0028
DSS
d0
d5
MLN DCs
MLN DCs
DSS, d0
DSS, d5
p100
p52
Gapdh
WCE

Figure 1

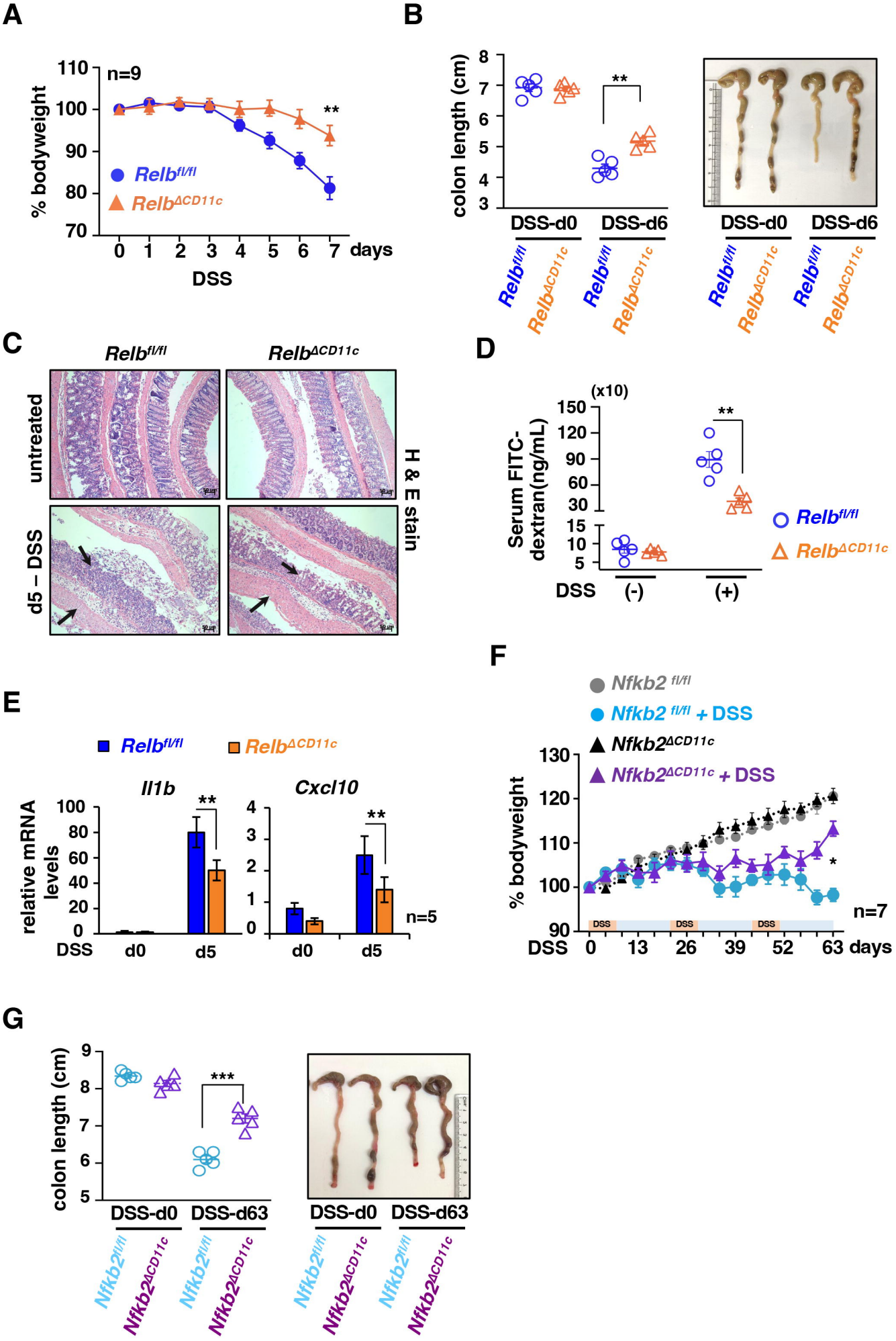
A
n=9
% bodyweight
110
100
90
80
70
**
Relbfl/fl
RelbΔCD11c
0 1 2 3 4 5 6 7 days
DSS
B
colon length (cm)
8
7
6
5
4
3
**
DSS-d0
DSS-d6
Relbfl/fl
RelbΔCD11c
C
Relbfl/fl
RelbΔCD11c
untreated
d5 – DSS
H & E stain
D
(x10)
Serum FITC-dextran(ng/mL)
150
120
90
60
30
15
10
5
**
Relbfl/fl
RelbΔCD11c
DSS
(-)
(+)
E
Relbfl/fl
RelbΔCD11c
Il1b
Cxcl10
relative mRNA levels
100
80
60
40
20
0
4
3
2
1
0
**
**
n=5
DSS
d0
d5
F
Nfkb2 fl/fl
Nfkb2 fl/fl + DSS
Nfkb2ΔCD11c
Nfkb2ΔCD11c + DSS
% bodyweight
130
120
110
100
90
*
n=7
DSS
0 13 26 39 52 63 days
G
colon length (cm)
9
8
7
6
5
***
DSS-d0
DSS-d63
Nfkb2fl/fl
Nfkb2ΔCD11c

Figure 2

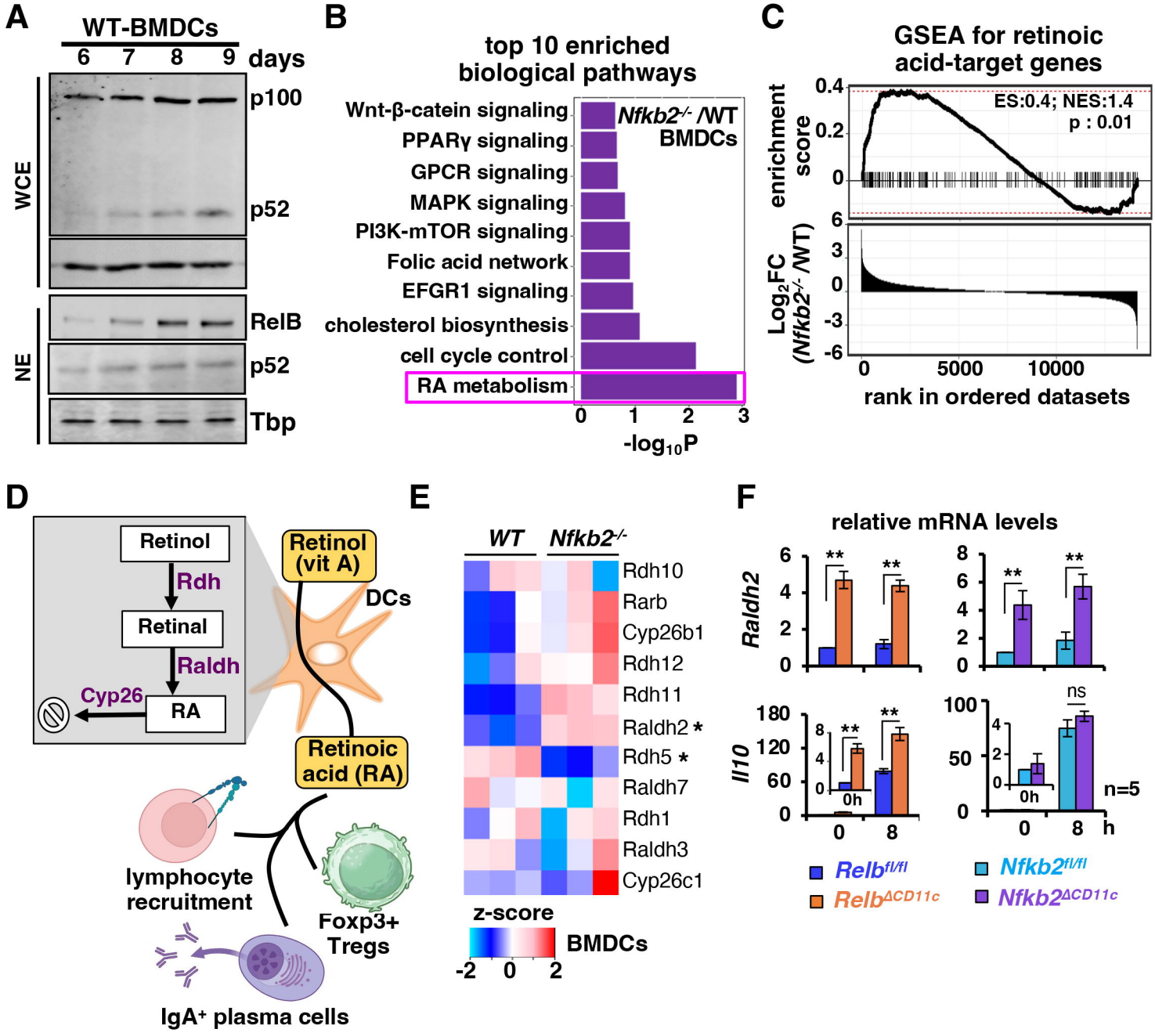
A
WT-BMDCs
6 7 8 9 days
WCE
p100
p52
NE
RelB
p52
Tbp
B
top 10 enriched biological pathways
Wnt-β-catein signaling
PPARγ signaling
GPCR signaling
MAPK signaling
PI3K-mTOR signaling
Folic acid network
EFGR1 signaling
cholesterol biosynthesis
cell cycle control
RA metabolism
Nfkb2-/- /WT BMDCs
-log10P
C
GSEA for retinoic acid-target genes
ES:0.4; NES:1.4
p : 0.01
enrichment score
Log2FC (Nfkb2-/- /WT)
rank in ordered datasets
D
Retinol
Rdh
Retinal
Raldh
Cyp26
RA
Retinol (vit A)
DCs
Retinoic acid (RA)
lymphocyte recruitment
Foxp3+ Tregs
IgA+ plasma cells
E
WT
Nfkb2-/-
Rdh10
Rarb
Cyp26b1
Rdh12
Rdh11
Raldh2 *
Rdh5 *
Raldh7
Rdh1
Raldh3
Cyp26c1
z-score
BMDCs
F
relative mRNA levels
Raldh2
Il10
0h
n=5
ns
Relbfl/fl
RelbΔCD11c
Nfkb2fl/fl
Nfkb2ΔCD11c
G
Relbfl/fl
RelbΔCD11c
Raldh2
Gapdh
WCE
Raldh2 levels
n=3
H
BMDCs
Relbfl/fl
RelbΔCD11c
Relbfl/fl+DEAB
RelbΔCD11c+DEAB
aldefluor
ΔMFI
n=3
I
Relbfl/fl
RelbΔCD11c
CD25
Foxp3
BMS493
% Foxp3+CD25+
n=3
Relbfl/fl
RelbΔCD11c
Relbfl/fl+ BMS493
RelbΔCD11c+BMS493

Figure 3

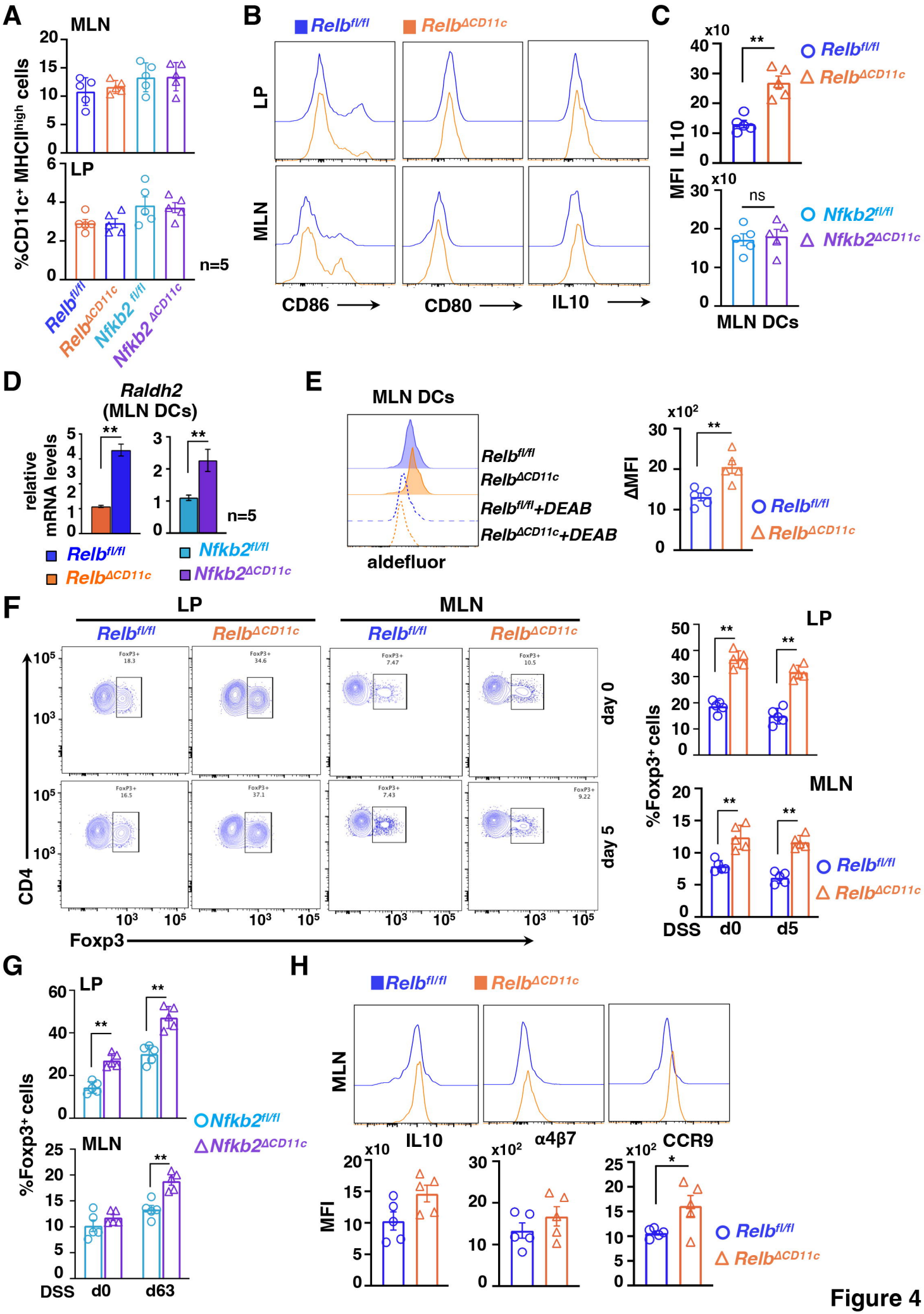
A
MLN
LP
%CD11c+ MHCIIhigh cells
n=5
Relbfl/fl
RelbΔCD11c
Nfkb2 fl/fl
Nfkb2 ΔCD11c
B
Relbfl/fl
RelbΔCD11c
LP
MLN
CD86
CD80
IL10
C
x10
MFI IL10
**
ns
Nfkb2fl/fl
Nfkb2ΔCD11c
MLN DCs
D
Raldh2
(MLN DCs)
relative mRNA levels
n=5
E
MLN DCs
Relbfl/fl
RelbΔCD11c
Relbfl/fl+DEAB
RelbΔCD11c+DEAB
aldefluor
x10²
ΔMFI
F
LP
MLN
day 0
day 5
CD4
Foxp3
%Foxp3+ cells
DSS
d0
d5
G
LP
MLN
%Foxp3+ cells
DSS
d0
d63
H
MLN
IL10
α4β7
CCR9
MFI
Figure 4

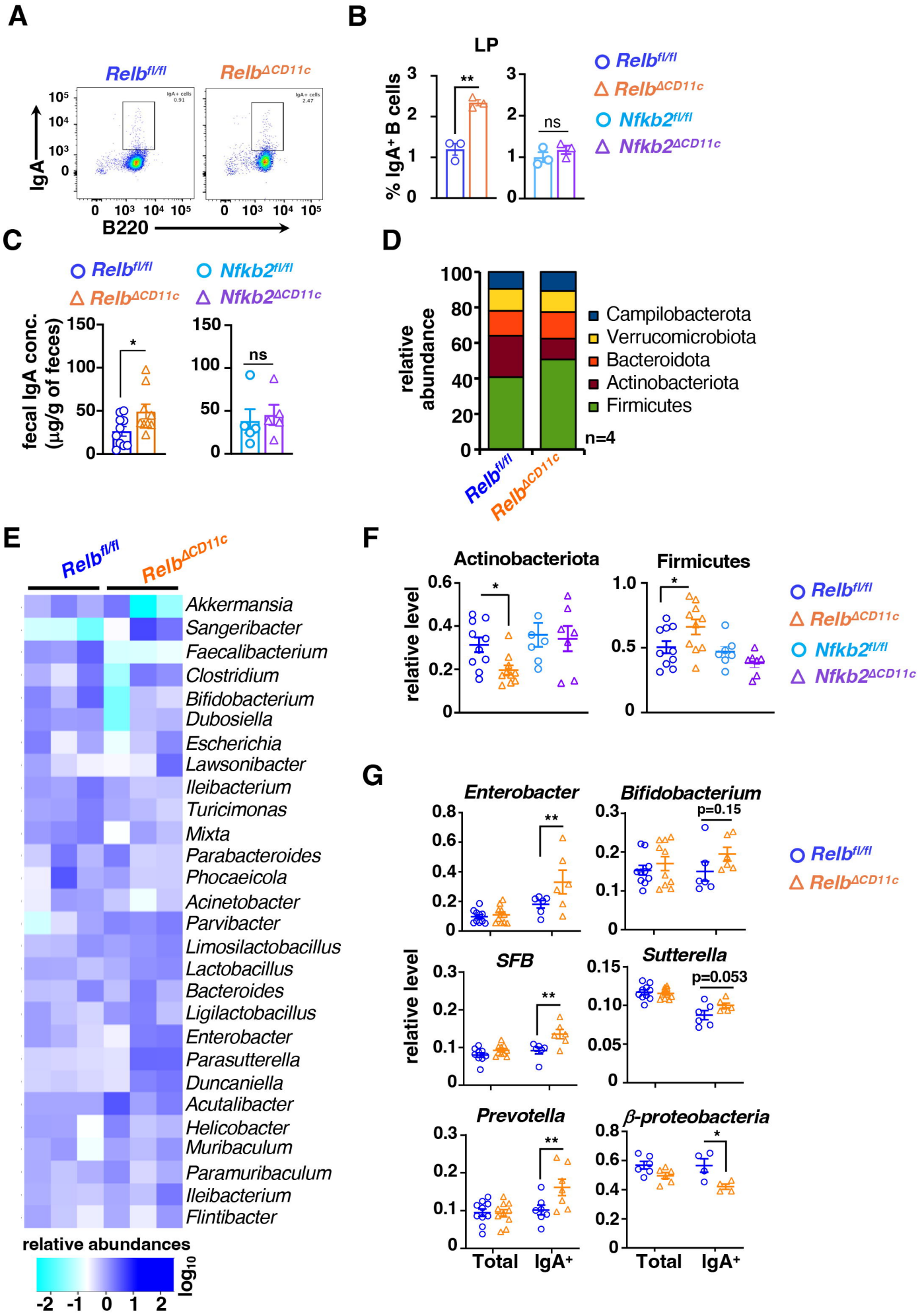
A
Relb fl/fl
Relb ΔCD11c
IgA
B220
B
LP
% IgA+ B cells
**
ns
Relb fl/fl
Relb ΔCD11c
Nfkb2 fl/fl
Nfkb2 ΔCD11c
C
fecal IgA conc. (µg/g of feces)
*
ns
D
relative abundance
Campilobacterota
Verrucomicrobiota
Bacteroidota
Actinobacteriota
Firmicutes
n=4
E
Akkermansia
Sangeribacter
Faecalibacterium
Clostridium
Bifidobacterium
Dubosiella
Escherichia
Lawsonibacter
Ileibacterium
Turicimonas
Mixta
Parabacteroides
Phocaeicola
Acinetobacter
Parvibacter
Limosilactobacillus
Lactobacillus
Bacteroides
Ligilactobacillus
Enterobacter
Parasutterella
Duncaniella
Acutalibacter
Helicobacter
Muribaculum
Paramuribaculum
Ileibacterium
Flintibacter
relative abundances
log10
F
Actinobacteriota
Firmicutes
relative level
G
Enterobacter
Bifidobacterium
p=0.15
SFB
Sutterella
p=0.053
Prevotella
β-proteobacteria
Total
IgA+

Figure 5

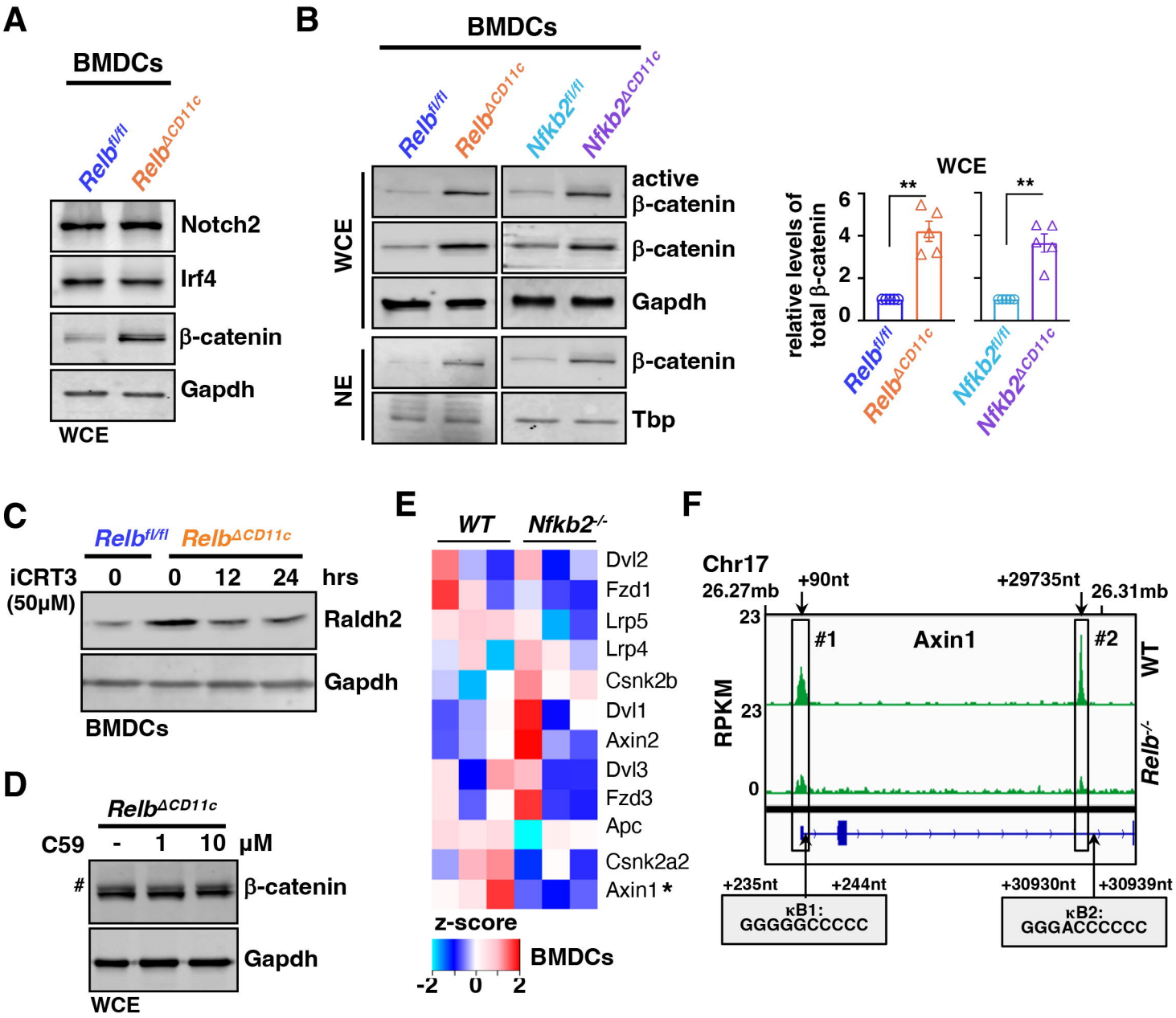
A
BMDCs
Relbfl/fl
RelbΔCD11c
Notch2
Irf4
β-catenin
Gapdh
WCE
B
BMDCs
Relbfl/fl
RelbΔCD11c
Nfkb2fl/fl
Nfkb2ΔCD11c
WCE
NE
active β-catenin
β-catenin
Gapdh
β-catenin
Tbp
WCE
relative levels of total β-catenin
6
4
2
0
**
**
Relbfl/fl
RelbΔCD11c
Nfkb2fl/fl
Nfkb2ΔCD11c
C
Relbfl/fl
RelbΔCD11c
iCRT3 (50μM)
0
0
12
24
hrs
Raldh2
Gapdh
BMDCs
D
RelbΔCD11c
C59
-
1
10
μM
#
β-catenin
Gapdh
WCE
E
WT
Nfkb2-/-
Dvl2
Fzd1
Lrp5
Lrp4
Csnk2b
Dvl1
Axin2
Dvl3
Fzd3
Apc
Csnk2a2
Axin1 *
z-score
-2
0
2
BMDCs
F
Chr17
26.27mb
+90nt
+29735nt
26.31mb
23
#1
Axin1
#2
WT
RPKM
23
Relb-/-
0
+235nt
+244nt
+30930nt
+30939nt
κB1: GGGGGCCCCC
κB2: GGGACCCCCC
G
relative mRNA levels
Axin1
1.5
1.0
0.5
0
**
**
n=5
Relbfl/fl
Nfkb2fl/fl
RelbΔCD11c
Nfkb2ΔCD11c
H
Relbfl/fl
RelbΔCD11c
Axin1
Gapdh
Relative Axin1 levels
1.5
1.0
0.5
0
**
Relbfl/fl
RelbΔCD11c
I
Input
IP: β-catenin
Relbfl/fl
RelbΔCD11c
Relbfl/fl
RelbΔCD11c
β-catenin
Axin1
GSK3β
#
+ MG132

Figure 6

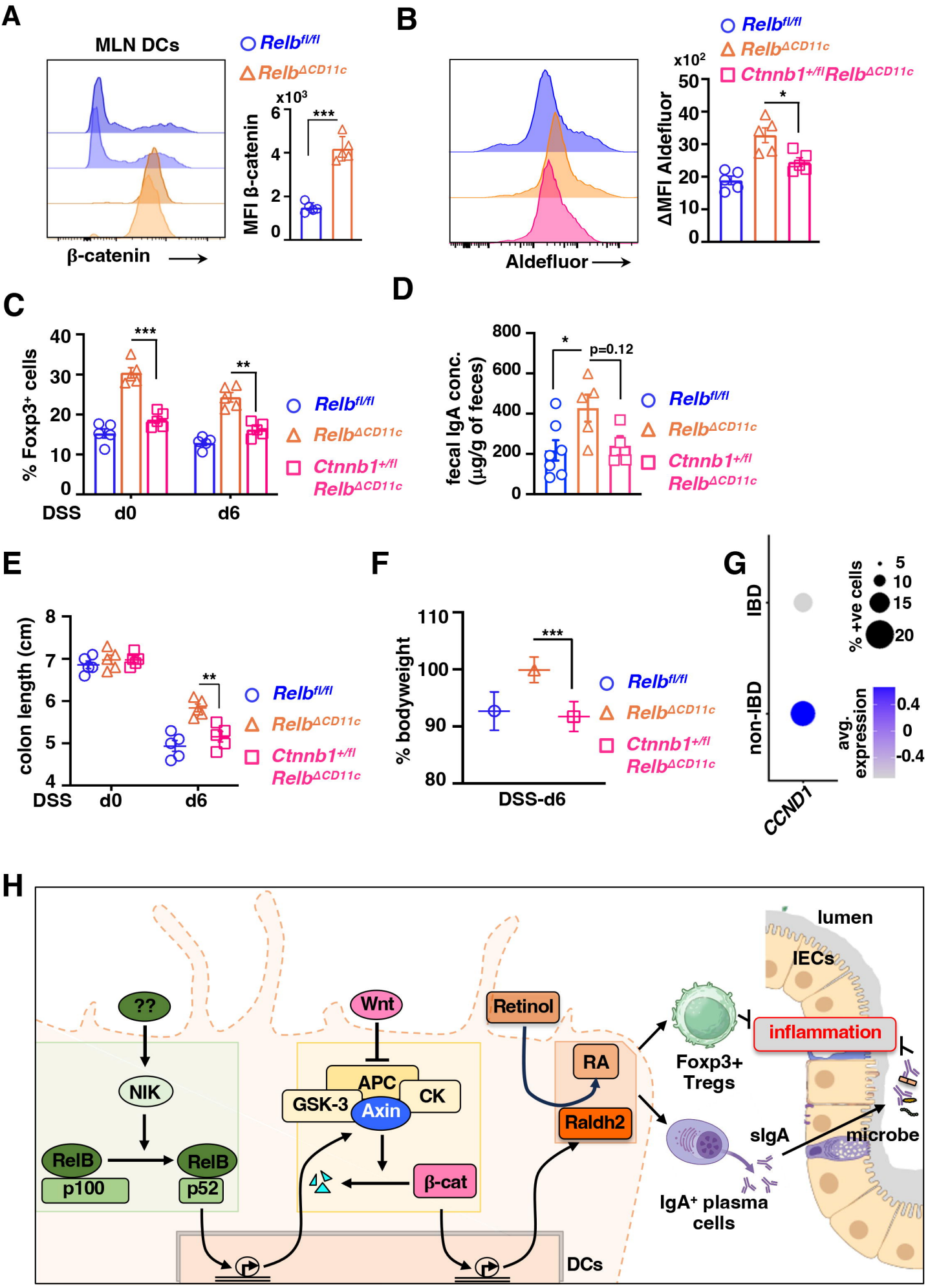
A
MLN DCs
Relbfl/fl
RelbΔCD11c
β-catenin
MFI β-catenin
x10³
***
B
Relbfl/fl
RelbΔCD11c
Ctnnb1+/flRelbΔCD11c
Aldefluor
ΔMFI Aldefluor
x10²
*
C
% Foxp3+ cells
***
**
DSS
d0
d6
Relbfl/fl
RelbΔCD11c
Ctnnb1+/fl RelbΔCD11c
D
fecal IgA conc. (µg/g of feces)
*
p=0.12
E
colon length (cm)
**
F
% bodyweight
***
DSS-d6
G
IBD
non-IBD
CCND1
% +ve cells
avg. expression
H
lumen
IECs
??
NIK
RelB
p100
p52
Wnt
APC
GSK-3
Axin
CK
β-cat
Retinol
RA
Raldh2
Foxp3+ Tregs
inflammation
sIgA
microbe
IgA+ plasma cells
DCs

Figure 7